Provided for non-commercial research and education use.
Not for reproduction, distribution or commercial use.

This article appeared in a journal published by Elsevier. The attached copy is furnished to the author for internal non-commercial research and education use, including for instruction at the authors institution and sharing with colleagues.

Other uses, including reproduction and distribution, or selling or licensing copies, or posting to personal, institutional or third party websites are prohibited.

In most cases authors are permitted to post their version of the article (e.g. in Word or Tex form) to their personal website or institutional repository. Authors requiring further information regarding Elsevier's archiving and manuscript policies are encouraged to visit:

http://www.elsevier.com/copyright

Author's personal copy

Computers & Fluids 39 (2010) 553–567

Contents lists available at ScienceDirect

Computers & Fluids

journal homepage: www.elsevier.com/locate/compfluid

Review

Inlet conditions for large eddy simulation: A review

G.R. Tabor [a,*], M.H. Baba-Ahmadi [b]

[a] School of Engineering, Mathematics and Physical Sciences, University of Exeter, Exeter EX4 4QF, UK
[b] Department of Aerospace Engineering, James Watt (South Building), University of Glasgow, Glasgow G12 8QQ, UK

ARTICLE INFO

Article history:
Received 19 December 2008
Received in revised form 10 September 2009
Accepted 16 October 2009
Available online 25 October 2009

Keywords:
Large eddy simulation
Inlet conditions
CFD

ABSTRACT

The treatment of inlet conditions for LES is a complex problem, but of extreme importance as, in many cases, the fluid behaviour within the domain is determined in large part by the inlet behaviour. The reason why it is so difficult to formulate inlet conditions is because the inlet flow must include a stochastically-varying component: ideally this component should 'look' like turbulence whilst at the same time be as simple as possible to implement and modify. We review methods for accomplishing this reported in the literature, these being 'precursor simulation' methods and 'synthesis' methods, and implement our own novel versions of these using the code OpenFOAM. Conclusions have been drawn about the relative merits of the different approaches, based on the physical realism of the results and the ease of construction and use.

© 2009 Elsevier Ltd. All rights reserved.

Contents

1. Introduction

Turbulence is a complex state of fluid motion, usually described in terms of pseudo-random coherent motions on a range of spatial and temporal scales superimposed on some 'mean' flow. The range of motions is fairly continuous between large scales determined by the geometry of the problem and small scales determined by the viscosity of the fluid, and this range is sufficiently wide that for most cases of interest, direct numerical simulation of the full Navier–Stokes equations (NSE) is impossible. Hence to solve turbulent flow problems we rely on turbulence modelling techniques, in which the number of degrees of freedom of the problem is substantially reduced by applying some averaging process: the resulting averaged Navier–Stokes equations are then solved together with modelled equations for quantities representative of the fluctuation around this average. Hence in Reynolds Averaged Navier Stokes (RANS) methods, an ensemble average is applied to the flow to divide it into a mean flow and fluctuations around this mean, which we choose to label as 'turbulence'. The RANS equations are then solved together with equations for quantities such as the turbulent kinetic energy k which are expected to be universal. Implicit within

* Corresponding author.
E-mail address: g.r.tabor@ex.ac.uk (G.R. Tabor).

0045-7930/$ - see front matter © 2009 Elsevier Ltd. All rights reserved.
doi:10.1016/j.compfluid.2009.10.007

Author's personal copy

this method is the assumption of a scale separation between 'turbulent' and 'non-turbulent' scales in the flow. In practise we often take the ensemble average to be equivalent to a time-average, and assume that the timescale for the fluctuations around the mean that we are labelling as 'turbulence' is considerably shorter than any timescale for variation of the mean flow, which may in fact be time-independent. Despite this RANS simulations have been remarkably successful, and can be considered as industry standard.

An alternative approach to turbulence modelling, which is gaining in popularity as increasing computational power makes it more accessible, is that of large eddy simulation (LES). Here the averaging applied to the flow is a spatial averaging in the form of a convolution with a spatial filter G, separating the flow into grid scale (GS) and sub-grid scale (SGS) components $\mathbf{u} = \bar{\mathbf{u}} + \overline{\mathbf{u}'}$, where $\bar{\mathbf{u}} = G * \mathbf{u} = \int_D G(\zeta, \Delta)\mathbf{u}(\zeta, t)d^3\zeta$, Δ is a characteristic scale of G, referred to as the filter width, and D is the computational domain. Conventionally we assume that the filter width is the same as the cell size Δx, hence the labels grid scale and sub-grid scale. In this case the averaged, or filtered Navier–Stokes equations take the form

$$\nabla.\bar{\mathbf{u}} = 0, \tag{1}$$
$$\partial_t\bar{\mathbf{u}} + \nabla.(\bar{\mathbf{u}} \otimes \bar{\mathbf{u}}) = \nabla.(\bar{\mathbf{S}} - \mathbf{B}),$$

given that the commutation $[G*, \nabla]\mathbf{u} = \mathbf{0}$: $\mathbf{u}$ is the velocity field, ν the molecular viscosity, $\mathbf{S} = -p\mathbf{I} + 2\nu\mathbf{D}$ with p the specific pressure, and $\mathbf{D} = \frac{1}{2}(\nabla\mathbf{u} + \nabla\mathbf{u}^T)$. The convolution process generates an additional term, the SGS stress tensor:

$$\mathbf{B} = \overline{\bar{\mathbf{u}} \otimes \bar{\mathbf{u}}} - \bar{\mathbf{u}} \otimes \bar{\mathbf{u}} = \mathbf{L} + \mathbf{C} + \mathbf{R}, \tag{2}$$

where $\mathbf{L}$ is the Leonard stress, $\mathbf{C}$ the cross stress and $\mathbf{R}$ the Reynolds-stress tensor (e.g. [22]). The term $\underline{\underline{\mathbf{B}}}$ represents the effect of the SGS turbulence on the GS flow. In classical LES these terms are replaced with explicit SGS models based on algebraic or transport equations for physical properties such as the SGS turbulent kinetic energy k. An alternative approach, implicit LES, relies on the numerical properties of the numerical differencing schemes to stabilise the simulation and substitute for the SGS stress tensor; no explicit SGS turbulence model being provided [17,16]. Recently, hybrid schemes such as detached eddy simulation (DES) [54] which blend LES for the free stream with RANS for the near-wall flow, have been proposed as another alternative. For the purposes of this review however there is little difference between these methods; the major problem with implementing LES inlet conditions lies in specifying the GS properties at the inlet, and these are simulated in exactly the same way in classical and implicit LES, and for the free stream of DES. Although our computational examples and most of the literature reviewed here uses classical LES, the inlet methods described should work equally with implicit LES and DES, although with the latter there may be additional complications with the blending at the walls.

There are several advantages of adopting the LES approach. In particular, no assumption is being made concerning scale separation. In fact, it is commonly assumed that the energy in the motions in the flow is continuously distributed in the conventional $-5/3$ power law spectrum of turbulence, and this energy spectrum is being truncated somewhere in the turbulent cascade, with the larger turbulent scales being explicitly simulated whilst the smaller, more universal scales are being replaced by the SGS turbulence model. Since we are often interested in the effects of the larger scales of the turbulence (but less often in the very smallest scales), then this leads to a more accurate representation of the transitory component of the flow, irrespective of whether we choose to label it 'turbulence' or not. However it does present problems when we need to apply boundary conditions. In RANS, because of the scale separation, all quantities specified on boundaries are constants, or at most slowly varying in time in comparison with the simulation timestep. In LES however, the GS variables always include some time-varying component, stochastically varying on all scales down to the spatial scale (the grid scale Δx) and the temporal scale (the timestep Δt) of the simulation. Put simply, at an inlet (and at a wall if wall functions are being used) turbulent fluctuations are present on the grid scale, and some method must be found for generating stochastic fluctuations in the grid scale quantities that 'look' like turbulence. Although in some problems (such as bluff-body flows), turbulence at the inlet is not a significant contribution to the turbulence within the domain, in a lot of cases the inlet conditions will have a significant impact on the flow dynamics, and thus the correct implementation of inlet conditions is of significant importance. In this paper we review various possible approaches to the problem, namely precomputed 'precursor simulation' techniques, and various approaches to synthesis of turbulence at the inlet. We also discuss comparative tests between the different methods, both from the literature and presenting our own results from LES of turbulent flow in a wall-bounded channel.

2. Inlet conditions used for LES

As emphasised above, generating inlet conditions for LES is considerably more difficult than it is for RANS. In theory we would want some or all of the following conditions to be met: the boundary should

- be stochastically varying;
- . . .on scales down to the filter scale (spatially and temporally);
- be compatible with the Navier–Stokes equations;
- 'look' like turbulence;
- allow the easy specification of turbulent properties (turbulence intensities, length scales, etc.);
- be easy to implement and to adjust to new inlet conditions.

There is a rough order of importance, or at least complexity, in the list above, in that it is relatively easy to implement a stochastically varying inlet (or even just a randomly varying one), much more difficult to ensure that it satisfies the Navier–Stokes equations.

What we mean by making it 'look' like turbulence needs some explanation; clearly one could create a wide range of flow fluctuations around the mean which would have specified spectral properties such as intensity and length scales (since these are integral properties covering the whole domain), and similarly could create a wide range of fluctuations which satisfy the Navier–Stokes equations. Not all would have the structure of turbulence, of coherent eddies across a range of spatial scales down to the Kolmogorov scale which interact with each other, and the issue of coherence in particular will turn out to be highly significant when trying to synthesise inlet turbulence (Section 3). Even the orientation of the eddies may be of importance if subsequent straining will occur within the computational domain. It is also important to distinguish between free stream turbulence and wall-bounded turbulence. For free stream turbulence we would certainly want to recreate the overall energy contained in the turbulent fluctuations; as well as this we might wish to recreate the distribution across length scales i.e. the spectrum, and single-point and two-point correlation functions, either because we have measurements for some of these properties, or because we believe them to be important for the physics we are attempting to simulate within the domain, or because they would be important for the incoming fluctuations to behave like turbulence. It is possible that the incoming turbulence in this case might be anisotropic, but it is probable that it would be homogeneous across the inlet. We may well also be able

Author's personal copy

to rely on Taylor's hypothesis to relate temporal and spatial distributions of turbulence. Wall-bounded turbulence however is significantly different from free stream turbulence, in ways which may be of importance for the inlet conditions. Most importantly, the structure of turbulence is modified significantly close to the wall, with it becoming anisotropic, two-dimensional, with vortex bursting from the laminar sublayer contributing to turbulence generation, and thus developing the well-known profiles of turbulent stresses with distance from the wall (measured in wall units, the structure collapsing to a universal profile, due to the law of the wall). As well as the mean flow profile as a function of distance from the wall, we are likely to need to generate the correct turbulent stress profiles τ_{xx}, τ_{yy} and τ_{xy} (x being the streamwise coordinate, y the distance from the wall); however other aspects of the turbulence may need to be modified, and for example Taylor's hypothesis may no longer be relied upon. In the case of a pipe inlet the radial pressure correlations may be important. Finally the inlet may need to integrate with any wall modelling used in the main domain, for example for detached eddy simulation (DES).

The final point, the ease of use, may or may not be more important than other issues (such as the compatibility with the NSE), but it is a significant one nevertheless. Existing methods described in the literature tend to fall into two basic categories: precursor simulation methods, in which some form of turbulence is precomputed before the main calculation and introduced into the domain at the inlet, and synthesis methods, in which some form of random fluctuation is generated and combined with the mean flow at the inlet. Both basic approaches have been recorded in the literature for some time; however in recent years a number of new variants have appeared. Comparisons between the different types are rarer in the literature; Keating et al. [35] have investigated the properties of precursor simulation methods and synthesis methods, together with a forcing method using control to drive the flow towards a pre-specified condition. Tabor et al. have also presented a similar group of comparisons [60]. Thus we feel it to be an appropriate moment to present a critical overview of the different methods, and this is the intention of this review article. The structure of the article is as follows: in Section 3 we present a review of the literature on synthetic inlets, in particular using Fourier series, digital filtering, principle orthogonal decomposition (POD) and vortex methods. In Section 4 we review the various implementations of the precursor simulation method. Section 5 starts with a discussion of comparisons between different techniques, summarising the findings of Keating et al., and presenting some computed results for the case of channel flow; then the review concludes with a discussion of the comparative merits of the different approaches.

3. Synthesised turbulence methods

One commonly-used method for generating turbulent inlets is to try to synthesise them according to particular constraints. At the simplest level this can involve introducing a white-noise random component to the inlet velocity, with an amplitude determined by the turbulent intensity level. This basic method is not an appropriate one; the white noise component has few of the required characteristics of turbulent flow – in particular it possesses no spatial or temporal coherence whatsoever – and so it is instantly destroyed by the Navier–Stokes solver. The inability of such a method to generate adequate inlet conditions has been demonstrated on several occasions [2,3]. In [3] a white noise inlet is compared with a more sophisticated precursor technique (see below for more details) for the canonical case of flow over a backward-facing step. The more realistic inlet condition is shown to trigger more rapid destabilisation of the mixing layer and thus produce a shorter mean recirculation length, and an increase in the frequency of vortex shedding. Mathey et al. [44] also investigate a white noise inlet as part of a comparison with the synthetic eddy method (see Section 3.3), finding that the white noise inlet overestimates re-attachment lengths by 50% and underestimates the spreading rate of shear layers. This is all attributable to the rapid damping of the non-physical fluctuations at the inlet leading to a low level of turbulence in the main flow; in the case of a shear layer the turbulence level is depressed by an order of magnitude.

However, the ability to synthesise the inlet would be valuable as it would be possible to parameterise the inlet conditions on a small range of adjustable parameters and thus easily create an inlet to a desired specification. More advanced synthesis techniques thus must concentrate on generating fluctuations which are more realistic, which must involve introducing spatial and/or temporal correlation.

3.1. Fourier techniques and related approaches

White noise fails as an inlet fluctuation because it lacks spatial and temporal coherence characteristic of true turbulence. Any more sophisticated approach must include this coherence. Turbulence is often analysed by decomposition onto a basis set, and in particular onto a basis set of harmonic functions, i.e. Fourier analysis. Thus, the turbulent fluctuations are represented by a linear sum of sine and cosine functions, with coefficients representing the energy contained in each mode. We can reverse the process, and write the turbulent fluctuation

$$u'_x(y) = u_m \sum_{i=1}^{N} a'_i \cos(i\kappa y + \varphi'_i), \tag{3}$$

(or equivalent rearrangements of the same basic relation). Here u'_x is the x-component of the fluctuating velocity, and y is some coordinate across the inlet to the domain. a'_i and φ'_i are coefficients to be determined from some form of constrained random process. This generates an arbitrary fluctuating profile which can be added to the mean velocity profile to generate an instantaneous flow profile

$$u_x(y,t) = \bar{u}_x(y) + u'_x(y,t) = \bar{u}_x(y) + u_m \sum_{i=1}^{N} a'_i(t) \cos(i\kappa y + \varphi'_i(t)).$$

The use of periodic functions provides spatial coherence across the inlet – in fact probably too much, as harmonic functions are coherent to $\pm\infty$; however this is unlikely to matter too much for a small inlet such as a pipe inlet. The selection of a'_i and φ'_i is important. a'_i relates to the energy contained in scales of wavenumber $i\kappa$, and by applying Parsival's identity, we have

$$\frac{1}{L}\int_{-L}^{L} \left[u'_x(y)\right]^2 \, dy = u_m^2 \sum_{i=1}^{N} \left(a'_i\right)^2. \tag{4}$$

Now we can time-average this. The l.h.s. is $2\times$ the turbulent kinetic energy in the x-direction flow been averaged in y-direction, so

$$2E_{k_x} = u_m^2 \sum_{i=1}^{N} \overline{\left(a'_i\right)^2}. \tag{5}$$

This demonstrates that the total turbulent kinetic energy E_{k_x} is related to the coefficients a_i. A prescribed power spectrum can be introduced to constrain the values selected for a_i. φ_i provides for phase differences between the modes, and for temporal phase shifts during the simulation. Hence, if a'_i and φ'_i are created from some random process as a function of time, the result will be a synthesised random field that evolves in a manner which can be precisely controlled.

The above synthesis has been presented assuming that the inlet is one-dimensional and only one component of the velocity has been treated. Of course the inlet will be two-dimensional, in which case we would need to extend the parameterisation, for example in Cartesian geometries:

Author's personal copy

$$u'_x(y,z) = u_m \sum_{i=1}^{N} a'_i \cos(i\kappa y + \varphi'_i) \sum_{j=1}^{N} b'_j \cos(i\kappa z + \varepsilon'_i). \quad (6)$$

In other geometries this becomes more complex, but in general solutions to the two-dimensional wave equation would give appropriate basis sets. For example, for a synthesis inlet for a cylindrical pipe, a combination of Bessel functions and Legendre polynomials would be appropriate. More difficult to solve is the problem of treating the different components of the flow. Fairly obviously the u'_x, u'_y and u'_z components can all be individually expressed in this manner, but in theory at least the different coefficients would need to be linked so as to generate the correct cross-correlation properties. In practice, this has not been done.

As an example, Lee et al. [42] use Fourier harmonics with coefficients selected to fit one of a selection of required energy spectra, for example

$$E(k) \sim k^4 \exp\left[-2\left(\frac{k}{k_0}\right)^2\right],$$

or the decaying spectrum

$$E^*(k^*) \sim k^*(1+k^*)\mathrm{e}^{-k^*} \quad \text{where} \quad k_i^* = k_i \alpha \sqrt{\nu(t-t_0)}.$$

The individual modes are combined with a random phase ϕ_r; to introduce temporal variation to the inlet, ϕ_r is allowed to shift by an amount $|\Delta\phi_r| < \Delta\phi_{max}$ within a time interval T_r. The temporal spectrum of the resulting turbulence could be influenced by the choices of T_r and $\Delta\phi_{max}$. The results show a good reproduction of the desired energy spectrum, and the paper also looks at time evolution and spacetime correlation of various quantities such as velocity derivative skewness and turbulent kinetic energy. Another example is the application of Fourier techniques to a compressible (Mach 0.75) jet by Andersson et al. [4]. This study demonstrated the importance of inlet conditions for real rather than idealised geometries, although some aspects of the work were concerned with compressibility effects.

It is essential to ensure that the synthesised fluctuations at least satisfy continuity. Development of temporal correlation is also critical to generation of realistic synthesised turbulence. Kondo et al. [38] attempt to match energy spectra and cross correlation information from experimental data, using a random Fourier series modified to satisfy continuity. Downstream of the inflow they found reasonable agreement for the required properties. Smirnov et al. [53] use a Fourier expansion with random coefficients taken from a Normal distribution $N(M,\sigma^2)$ to generate an isotropic random field [40], with an energy spectrum of the form

$$E(k) \sim k^4 \mathrm{e}^{-2k^2}.$$

This is then subjected to a time-dependent scaling transformation based on the correlation tensor of the target field r_{ij} and information about the length and time scales of the turbulence, e.g. from a steady state RANS simulation or from experimental data. The resulting flow field has the correct statistical properties and is also divergence free. They validated their method by generating homogeneous isotropic flow fields and also anisotropic boundary layer flows, then successfully applied the method to LES of a ship wake. One useful feature of this method is that it can also be used to generate an equivalent random initial field to initialise the simulation. This spectral synthesis method is implemented in the commercial code fluent.

Davidson [13] generates a collection of realisations of the inlet turbulent field using superposition of Fourier modes with random phases and constrained random amplitudes, constrained to match a prescribed energy spectrum (a modified Karman spectrum in this case). Temporal correlation is provided at each timestep by creating a linear interpolation of the running average of the inlet profiles with the next realisation. The method is validated for hybrid LES-RANS of channel flow at $\mathscr{R}e_\tau = 2000$. He finds the imposed time scale to be more significant in generating useful inlet turbulence, and also that inlet time and length scales should be related to the grid properties rather than to the actual values, and suggests that such synthesis methods should be seen as generating not actual turbulence, but fluctuations that can be important in triggering turbulence downstream of the inlet. Another approach to generating temporal correlation is through the use of stochastic random processes. Tabor et al. [60] link the coefficients of a Fourier series a_i, φ_i to an Ornstein–Ubbink (OU) process, which generates Gaussian-distributed random numbers with prescribed mean and variance and temporal correlation. The average magnitude of a_i can be controlled to fit a desired turbulence spectrum ($E(k) \sim k^{5/3}$ was used), and the temporal correlation controlled to provide a degree of temporal correlation on the inlet fluctuations. It is also possible to generate fluctuations using other basis sets. This would certainly be necessary for more complex inlet geometries; the basis set should reflect the properties of the flow at the edge of the boundary, for example if the inlet flow is coming through a pipe the basis functions should all be zero at the circumference of the pipe. For a circular pipe this would suggest the use of Bessel functions, whilst for more complex shaped openings it may be necessary to generate a basis set from solving Laplace's equation in two-dimensional. Returning to the simple rectangular case, the use of wavelet series may show some potential. Wavelets are basis functions with compact rather than infinite support, and allow the decomposition of an input signal into frequency and domain information rather than just frequency information. In this context, they would allow the synthesis of velocity fluctuations with local correlation rather than the infinite correlation generated by harmonic functions. An example of this is provided in Section 5 below.

3.2. POD methods

Principal orthogonal decomposition (POD) analysis has been applied as a way of analysing turbulence in general. POD takes as input an ensemble of instantaneous realisations or snapshots and extracts basis functions optimal for the representation of the data;

$$u(\mathbf{x},t) = \sum_{n=1}^{N} a^{(n)}(t)\phi_t^{(n)}(\mathbf{x}),$$

decomposing the data into spatial and temporal eigenvectors. Usually we find that only a small number of the basis functions are sufficient to reconstruct the majority of the information in the dataset. Thus this represents a good way of extracting information about the largest scale coherent structures in the flow. Working this backwards, coupling with some kind of stochastic or random process, should in theory construct high-quality synthetic turbulence for an inlet. Drualt et al. [18] have applied this to generate inlet conditions for both DNS and LES from experimental data acquired using hot wire measurements, and for two-dimensional and three-dimensional DNS from precursor DNS data. Hot wire measurements provide good temporal resolution of the data but spatial resolution is a problem, being restricted by the number of probes that can be utilised simultaneously, so the authors are forced to use linear stochastic estimation to fill in the gaps between the measured location. Nevertheless, good results are found using a minimum size of relevant information. Perret et al. [46,47] have taken the same approach using stereoscopic PIV measurements to provide inlet conditions for LES of a mixing layer. PIV has the opposite problem to hot wire; large quantities of spatial data is available, but the flow is under-resolved temporally, which the authors are forced to compensate for by introducing a synthetic random time series. One- and

Author's personal copy

two-point statistics for the synthesised fields are compared with those measured, with generally satisfactory results. The synthesised velocity fields exhibit correct energy levels and spatial partition, and anisotropy of the flow and shear stress are well reproduced, as are the two-point correlations. However long range correlation levels are over-predicted; and typical frequencies of the mixing layer found from hot wire measurements are not present in the data. Results from the LES are affected by this; the synthesis of the time series data is not perfect and a significant adaptive section is present downstream of the inlet as the inlet flow evolves towards true turbulence, although as the authors observe, the use of simple Gaussian random fluctuations would have lead to an immediate relaminarisation of the flow. A similar approach was used by Johansson and Andersson [34] who used a Galerkin projection of the NSE onto the most energetic modes from a POD of the target flow. They found it necessary to add low-energy, small-scale POD-modes to the primary modes in order to more rapidly establish the correct level of dissipation and achieve a more realistic distribution of energy between the velocity components.

3.3. Other methods

Another synthesis approach involves generating entirely random number data which can then be processed using digital filters to generate desired statistical properties such as spatial and temporal correlation [15,37,43]. Further transformations are then applied to generate anisotropic turbulence matching a specified Reynolds-stress tensor. The method is thus a generalisation of that used by Lee et al. described above [42] and Smirnov et al. [53]; but where these authors use random Fourier series to produce the initial random data, di Mare and Klein use digital linear nonrecursive filters. Thus, if r_m is a series of random data with zero mean and unity variance, then

$$u_m = \sum_{n=-N}^{N} b_n r_{m+n},$$

which is a convolution or digital filter, introduces correlation between successive realisations of the data. The quantity u_m can be interpreted as being the value of one component of the velocity vector at a single-point in the inlet; N represents the support of the filter, and b_n are the filter coefficients. N and b_n are thus related to the correlation between neighbouring points, and a relationship can be derived between the filter coefficients and the two-point velocity correlation function:

$$\frac{\langle u_m u_{m+k}\rangle}{\langle u_m u_m\rangle} = \frac{\sum_{j=-N+k}^{N} b_j b_{j-k}}{\sum_{j=-N+k}^{N} b_j^2}. \tag{7}$$

The methodology can be simply extended to three-dimensional by regarding the three-dimensional filter as an outer product of three one-dimensional filters; thus

$$b_{ijk} = b_i \dot{b}_j \dot{b}_k.$$

The only serious obstacle to using this is then how to invert Eq. (7), particularly given that the information available about the correlation function may be quite limited. However it seems likely that the method will be insensitive to the detailed function, so an exponential decay with a specified length scale is adopted. The resulting methodology is applied to LES of a plane jet and a boundary layer [15] and DNS of plane jet and jet breakup [37]. di Mare et al. demonstrate two versions of the method; a simplified method matching Reynolds stress and a single length scale, and a more complex variant which seeks to reproduce the complete Reynolds-stress tensor, which they find reproduces well much of the structure of the flow and provides a closer match to DNS results, particularly for wall-bounded flows.

The digital filter method described above is basically an implementation via digital filters of a Gaussian stochastic process. This suggests that other variants could be generated using different filtering techniques. Veloudis et al. [63,62] discuss this in the context of the impact of non-uniform meshes on the technique; for a uniform mesh a single filter coefficient b_{ijk} is probably sufficient, but if the turbulent scales vary across the inlet plane, a variation which in LES may be linked to the LES filter width and hence the mesh, a range of filters may be required, which complicates the method and increases its computational cost. They investigate multi-filter approaches, including methodologies for reducing the computational cost, and apply their results to flow in a constricted channel. Reasonable results are obtained for the mean velocity profiles, compared with literature LES results [61]; results for the various Reynolds stress components are more mixed. Xie and Castro [67] use another digital filtering technique to generate inlet conditions for street-scale flows, with good results.

Finally in this section, a recent approach to inlet synthesis is the vortex method or synthetic eddy method (SEM). This is based on a Lagrangian treatment of vortices, which are generated with a given vorticity distribution at the inlet and transported into the domain from there. Benhamadouche et al. report on the development of this method [10], based on an earlier PhD thesis by Sergent [52]. They create two-dimensional vortices for the lateral components of the fluctuating velocity and use a one-dimensional Langevin equation for the streamwise component. The method has been implemented in the commercial code Fluent and tested on a range of test cases including pipe and channel flow, aerofoil flow and flow over a hill [44,32], and for indoor flows [1]. Comparison [32] with other synthesis methods (a Fourier synthesis method [8] and Lund's method [43]) is favourable with the SEM needing a substantially shorter length of domain downstream of the inlet to develop realistic turbulence.

4. Precursor simulation methods

The other method that has been used to generate inflow conditions involves running a separate, precursor, calculation of an equilibrium flow to generate a 'library' of turbulent data which can be introduced into the main computation at the inlet. This has the advantage that the inflow conditions for the main computation are taken from a genuine simulation of turbulence, and thus should possess many of the required characteristics, including temporal and spatial fluctuation with correlation and a correct energy spectrum. The library itself can be generated in a number of ways, for example using periodic boxes of turbulence or cyclic channel flow calculations in which either periodic boundary conditions can be used, or recycling arguments can be invoked. Then, the velocity field in one plane normal to the streamwise direction is stored at each time step. The sequence of planes is then read in as inflow data for a separate calculation of the flow of interest. Note that the precursor simulation does not need to be at the same Reynolds number. It is only supposed to provide some reasonably realistic scales that will, presumably, develop quickly into the eddies appropriate to the particular flow in the LES region. Generally the precursor domain will be of the same cross-section as the inlet itself, so complex shaped inlets will be no more difficult than simple rectangular ones.

4.1. Cyclic domains

In many cases we wish to compute fully-developed flow. For example, flow in a channel bounded by flat-plates is a canonical case for turbulent flow simulation research; given a long enough entry section, experimental results settle down to give flow

Author's personal copy

profiles which are invariant in the streamwise direction. These flow profiles have been measured very accurately, and so this serves as a good case to compare computational results against. Similarly, flow in a long pipe becomes fully developed sufficiently far downstream from the inlet (the mean velocity profile becoming invariant after about 40D downstream from the inlet, where D is the pipe diameter; Reynolds stress components require a longer distance to develop further but eventually become invariant in the streamwise direction). Experimentally, a long enough pipe section to achieve fully-developed flow is relatively simple to achieve. Computationally, providing a long enough pipe section would be prohibitive. However it is unnecessary to do this. If flow out of the outlet of the domain is reintroduced directly into the inlet through some sort of mathematical mapping, then the flow recirculates through the same domain endlessly, and will quickly arrive at a fully developed state. Using such a domain it is possible to study fully-developed flow using quite a short section of the channel or pipe, constrained only by the periodicity inherent in the technique. Such cyclic domains have been extensively used in fundamental studies of LES and DNS, and in the study of wall-bounded turbulence (e.g. [20,41,36]).

Many early simulations of spatially developing turbulent flows with turbulent inlet attempted to use modifications of the periodic conditions to manipulate the data. Spalart [55,56], for instance, performed DNS of sink-flow boundary layers and flat-plate boundary layers using periodic boundary conditions. To account for the variable boundary-layer thickness (decreasing in sink-flow, increasing in the flat-plate case) he used source terms in the equations that served to transform the equations into a self-similar coordinate frame, in which the flow was periodic. Since such similarity does not always occur, Spalart and Watmuff [57] proposed a modification of this method, where a fringe region was appended to the end of the domain, in which forcing terms were added to the equations for motion to decrease the boundary-layer thickness, and re-establish an equilibrium boundary layer. Periodic boundary conditions could then be used to reintroduce the outlet velocity field at the inlet. In this context, some authors distinguish between a channel with periodic boundary conditions between its ends, and *recycling*, in which the flow is sampled at some location in the domain and the resulting information reintroduced at the inlet.

Also of interest are attempts to generate flow with prescribed bulk properties, most notably swirl. Swirl injectors are important in combustion, and so LES of swirling flow is a significant area of research. Pierce and Moin [48] present a methodology for generating swirl within a cyclic channel by imposing a constant tangential body force on the flow. They use constant, linear and quadratic profiles

$$f_\theta = F, \quad F\left(\frac{r}{R}\right), \quad F\left[1 - 4\left(\frac{r}{R} - \frac{1}{2}\right)^2\right],$$

to generate swirl in pipes, and a similar set of functions for swirling annular flow. Simulation in a spatially periodic domain conveniently generates a fully developed, swirling flow.

4.2. Preprepared library

Cyclic domains are valuable tools in their own right, enabling the computation and study of fully-developed flow in a short domain space. For the purpose of this review however their main utility is in generating turbulence data which can be used for a precursor simulation approach. It is relatively straightforward to sample the data at a prescribed location in the auxiliary computational domain, and save the results for introduction into the main domain inlet, particularly when the auxiliary computation can be modified to match the desired conditions of Reynolds number and mesh structure – the one to ensure the proper turbulent flow, the other for computational simplicity. Simulations using these methods show good agreement with experimental measurements, and typically the flow entering the domain is correctly turbulent; no further development section is necessary. However they still require the generation and storage of a separate database. Since this is of finite extent, it will introduce periodicity into the computation which may significantly affect any statistical properties being computed. This point has been examined by Chung and Sung [12], who examine several different methods for mapping data from a precursor simulation of a cyclic channel to a main simulation of a similar channel. These include a temporal database as described above, and a spatial database created by sweeping the cutting plane through a single timestep of the precursor simulation an applying Taylor's hypothesis (this however has the flaw that the flow velocity varies with distance from the wall and thus Taylor's hypothesis is not strictly valid). In addition they examine ways of manipulating the data via amplitude and phase 'jittering' [42], introducing random fluctuations into the data, in order to destroy the periodicity in the database. Results are not completely convincing, with each of their methods demonstrating significant and distinct problems. Similar techniques have been applied to cylindrical pipes [59].

Another example of this method has been developed for hybrid RANS/LES simulations by Schluter, Pitsch, and Moin [51]. They used a precursor database to provide turbulent fluctuations which were then rescaled according to the Reynolds stress predicted by a RANS calculation, and imposed on the target mean profile also obtained from RANS. However, little is known about the effect of the significant rescaling that occurs when the database is very different from the target turbulent field, not to mention the issues related to superposition of the turbulent fluctuations on the mean profiles. Such simulations are found to require an adaptive length downstream of the inlet where flow conditions return to full turbulence.

Precursor databases are extensively used for LES of swirling flows [66,25], based on the work mentioned above by Pierce and Moin on swirl in cyclic channels [48]. As an example of this, Wang and Bai [65] use Pierce and Moin's method to create a 10,000 timestep library for lookup which is then cycled through as appropriate. The library however does not meet the specifications for the required flow, and so the data is rescaled to meet the desired statistical properties (specified mean and variance of velocity). However this rescaling does cause problems; the level of turbulent kinetic energy is seen to decrease downstream of the inlet, which the authors attribute to the unphysical turbulence at the inlet adapting to become true turbulent flow further downstream. Schlüter et al. [50] also implement and compare various inlet conditions for swirl, specifically a laminar inflow (no fluctuations), inflow with random fluctuations, and various precomputation methods. As before, the laminar and random fluctuation techniques produce poor results, whilst the various precursor simulation techniques perform much better. García-Villalba et al. [26] use this method in two of the three methods that they compare for an annular swirling jet discharging into a free domain. In their work; Sim 1 uses a constant velocity inlet including a swirl component far upstream of the jet discharge; Sim 2 uses a precomputed database to provide inlet conditions at the jet discharge point, and Sim 3 introduces these conditions some distance upstream of the discharge point, thus allowing some distance for the turbulence to develop, but not as far upstream as for their case Sim 1. They find significant differences between the computed flows between the different cases, not just in terms of detailed parameters such as rms. flow profiles, but also in terms of gross structures, and in particular the large scale unsteady flow structures. They adopt the methodology of Sim 3 for subsequent work investigating the dependence of coher-

Author's personal copy

ent structures on the presence of a pilot jet and the level of swirl [25]. However in other work [27] they adopt the methodology of Sim 1 for the inlet, claiming that the turbulence develops adequately for their purpose in the inlet section to the domain, although they do admit that this is not an ideal approach for LES.

4.3. Concurrent library generation

A modification of these precursor methods is to run the precursor calculation continuously in parallel with the main simulation, essentially computing 'on the fly' the data to be used in the simulation. Such a technique was originally proposed by Lund, Wu, and Squires [43]. This method, which was developed for flat-plate boundary layers, consists of taking a plane of data from a location several boundary-layer thickness δ downstream of the inflow, and rescaling the inner and outer layers of velocity profiles separately, to account for the different similarity laws that are observed in these two regions. The rescaled velocity profiles are then reintroduced at the inlet. Ferrante and Elghobashi [19] proposed a more robust variant of the method of Lund, Wu, and Squires [43]. Using direct numerical simulation, they were unable to obtain a satisfactory development of the boundary layer using the method by Lund, Wu, and Squires [43] (which was tested using large eddy simulations). They corrected this by initialising the flow in the rescaling region using the method of Le, Moin, and Kim [43], which prescribes the Reynolds-stress tensor and the energy spectra.

Both the fringe method [57] and the rescaling by Lund, Wu, and Squires [43] have been applied in LES and DNS. Their main shortcoming is the fact the inlet must be placed in a region in which the flow is in an equilibrium, well-known condition (flat-plate boundary layer, for instance) and a fairly long domain must be used for the region of interest for the recycling. Apart from the increased cost of the calculation both in terms of computational time and memory requirement, this introduces two additional difficulties: the fact that, in some flows, an equilibrium region in which scaling arguments can be applied may not exist at all, and that recycling may introduce spurious periodicity into the time series.

4.4. Internal mapping

One disadvantage of all these methods is the necessity to set up and run a separate calculation involving a separate mesh, either *a priori* or concurrently with the main computation. However there is actually no reason why the precursor calculation cannot be integrated into the main domain, with sampling downstream of the inlet being mapped back into the inlet. It is of course necessary to provide some mechanism for driving the flow in this case, which can easily be provided by correcting the mapped velocities to ensure a constant target flux [14,60]. An example is included in the comparative tests demonstrated below Section 5.1. Other possibilities are to introduce velocity corrections within the inlet section, or introduce an artificial body force into this region, both coupled to control algorithms to drive the flow towards a pre-specified target [5,7]. Such an approach can also generate swirl [6,5].

5. Analysis

In this section we attempt to draw some conclusions about the different inlet conditions described above. The most valuable study of inlet conditions for LES would be one which implements all the above inlet methodologies in the same code with the same modelling (SGS, numerical, etc.) and compared them with each other on a standard test case. This has rarely been done. The best example of this is the work of Keating et al. [35], which compares the following four methods:

(1) a precursor database,
(2) a Fourier synthesis method [8,9],
(3) rescaling fluctuations from a lower Reynolds calculation [51],
(4) synthetic turbulence generation with controlled body forces applied at discrete planes [58].

They find that although the Fourier synthetic method tested (2 above) does generate fluctuations with a realistic spectrum, and takes into account near-wall anisotropy in the flow, it still requires a significant length downstream of the inlet for true turbulence to develop. The length of the transition region appears to be linked to the rapid decay of wall-normal fluctuations in the channel centre. Introducing the controlled body forcing (4) improved this and was found to give good results. This forcing was used to enhance wall-normal fluctuations at discrete locations using a control algorithm based on the difference between the calculated Reynolds shear stress and the target profile. Wall-normal fluctuations are enhanced over the entire channel height. Although a development section is still necessary for the development of actual turbulence, the necessary section is considerably shortened, with the error in the Reynolds shear stress reduced to acceptable values within five channel half heights, although the correct friction coefficient and turbulent kinetic energy values take somewhat longer to achieve.

Results from their preprepared library methods are similarly informative. For the precursor simulations (1), a baseline simulation case was performed to generate validation data, and planes of velocity data saved to disk to generate a time series of length $78\delta/U_b$ (δ being the channel half-width) which could be used as inlet data for the main domain. They observe that the storage of a much longer time series would be impractical, and estimate that an increase in the length of the time series by a factor of 4 would be necessary to achieve error levels less than 4%. The inlet velocity database was also filtered using both high-pass and low-pass filters before use to determine which length scales are most important in the redevelopment of turbulence downstream of the inflow plane. They find that the large scales (size larger than the integral length scale L) are the most important. Flows which were filtered to remove scales larger than L rapidly relaminarised. Flows which retained these scales but filtered to remove extremely large eddies (scale $\geqslant 4L$) were found to regenerate turbulence eventually, but it did require a significant distance for this process to occur. Finally, the recycling method used (method 3) introduced turbulence with realistic time and length scales; however the case tested was significantly different in Reynolds number from the actual calculation setup, and the necessary rescaling resulted in a fairly long development length being needed. This development length was found to be intermediate between the controlled forcing and the synthetic turbulence methods, but the errors in this section were small and might be regarded as acceptable.

Grinstein [29] includes a discussion of many of the issues relating to LES inlet conditions, including the observation that there is not unique reconstruction of an unsteady velocity field using turbulent eddies based on single-point statistical correlation data. He recognises that many inlet conditions do no more than provide a trigger for the development of true turbulence within an inlet section, but points out that the possibility of including such an inlet section may be constrained by the physical geometry being simulated, e.g. in the case of combustor flows with swirl inlets [21]. He also discusses the importance of inlet conditions in urban canyon modelling, where contaminant transport is strongly influenced by inlet wind gusts [45], although observing that the impact of the inlet conditions is reduced downstream of the first structure in the domain. Gilling et al. examine the application of various types of synthetic and precursor calculations to spatially decaying homogeneous turbulence and to flow around an aerofoil. They find,

Author's personal copy

unsurprisingly, that the more realistic the inlet turbulence, the closer the decay rate is to the theoretical expectation. For the aerofoil, the flow is sensitive to the inlet turbulence, with simulations with better resolved inlet turbulence being closer to the experimental results, particularly when determining lift and drag around stall. This is because separation can be triggered by the upstream turbulence.

5.1. Comparative examples

Tabor et al. [60] presented a similar survey of inlet conditions at the 2004 ECCOMAS conference. Some of these results are reproduced here for illustrative purposes. As with the work of Keating et al. [35], the case being simulated is that of fully-developed flow between two flat-plates separated by a distance $2d$ – a channel flow problem (d being the channel half-width). We compare with DNS data published by the Kasagi–Suzuki/Shikazono Lab [31] which provides profiles of velocity and higher moments for various Reynolds numbers, and with LES data from shorter, cyclic channels [22]. The geometry consists of a domain of 20 m in length between two flat-plates 2 m apart, as shown in Fig. 2; the channel is therefore 10 channel-widths in length or 7900 wall units in length. The inlet flow velocity and fluid viscosity are arranged to create a flow at Reynolds number $\mathscr{R}e = 13,750$ based on the channel half-width, equivalent to a friction Reynolds number $\mathscr{R}e_\tau = 400$ based on the friction velocity. The flow is in the x-direction, and the domain boundaries are symmetry planes at $z = 0$ and $z = 2$ m, giving (in effect) an infinite domain in this direction. The mesh is generated from two blocks in the y-direction, allowing mesh grading towards the walls coupled with van Driest damping to deal with the near-wall flow. The mesh resolution is $60 \times 50 \times 30$ $(x \times y \times z) = 90,000$ cells, with the first near-wall layer of cells being of width $\Delta y^+ = 2$, a resolution which has been found to give good results [20].

The filtered Navier–Stokes Eq. (1) together with (2), are solved using the CFD code library OpenFOAM. This is a C++ code library of classes for writing CFD codes, which includes a well-tested and validated LES capability [22,20,23,24]. Eq. (1) are discretized using the finite volume method, where the domain D is divided into cells δV_i so that $\bigcup_i(\delta V_i) = D \cup \partial D$ and $\bigcap_i(\delta V_i) = \emptyset$. Integration of the dependent variables over each cell δV_i, together with application of Gauss' theorem, generates a set of discretised equations with the divergence terms in Eq. (1) represented as fluxes across the cell faces, evaluated using appropriate interpolation schemes; we use centred second order interpolation and NVD-derived interpolation (gamma scheme, see [33]). Time integration is carried out by the Crank–Nicholson scheme, which is second order in time. Following the procedure of Rhie and Chow [49], discretisation of the ∇p term is left; a Poisson equation is constructed which implements the incompressibility condition $\nabla \cdot \bar{\mathbf{v}} = 0$, and the equation set solved sequentially using the resulting PISO algorithm [30]. Solution is performed implicitly by matrix inversion using Incomplete Cholesky Conjugate Gradient methods. The SGS tensor, Eq. (2), is modelled using the standard Smagorinsky model, where

$$\mathbf{B} = \frac{2}{3}k\mathbf{I} - 2\nu_k\overline{\mathbf{D}}_D.$$

Here, $\overline{\mathbf{D}}_D = \overline{\mathbf{D}} - \frac{1}{3}\mathrm{tr}\overline{\mathbf{D}}\mathbf{I}$, and the sub-grid quantities k (the SGS turbulent kinetic energy) and ν_k (the sub-grid turbulent viscosity) are evaluated, assuming a $-5/3$ power spectrum, using the relations

$$k = C_I\Delta^2\|\overline{\mathbf{D}}\| \quad \text{and} \quad \nu_k = C_D\Delta^2\|\overline{\mathbf{D}}\|,$$

and the model coefficients are $C_I = 0.202$ and $C_D = 0.042$. All of this is implemented within OpenFOAM and operates on an arbitrary unstructured mesh.

Four different inlet conditions have been implemented and compared, as follows:

- A precursor simulation technique using data taken from a prior calculation on a short section of channel computed with cyclic boundary conditions and an internal body force to drive the flow. Data from the centre plane of the calculation is saved at each successive timestep for a period equivalent to 10 complete flow transits of the domain, to create this dataset for the calculation. We will refer to this as method I – precursor simulation.
- A fourier series technique. In this the fluctuating velocity is represented by the series (3) with the coefficients a_i' and φ_i' given values from a stochastic OU process. The parameters of this process are chosen so that the resulting fluctuations match a prescribed energy spectrum $E(k) \sim k^{-5/3}$ and provide an appropriate degree of temporal correlation.
- A second, related synthesis method is implemented, using wavelets rather than harmonic functions as the basis set. We introduce turbulent fluctuations $u'(y)$ in form the inverse wavelet transform based on the discrete wavelets as follows:

$$u'(y) = \sum_j \sum_k \alpha_{j,k}\psi_{j,k}(y), \tag{8}$$

where $\alpha_{j,k}$ and $\psi_{j,k}(y)$ are wavelet coefficients and discrete wavelets respectively, defined as follows:

$$\alpha_{j,k} = \int_\infty^\infty u'(y)\psi_{j,k}^*(y)\,dy, \tag{9}$$

$$\psi_{j,k}(y) = 2^{j/2}\psi(2^j y - k), \quad (j,k \in Z), \tag{10}$$

where ψ is mother wavelet, j is the scale parameter, k is the shift parameter and Z is the set of all integers. In this case the Meyer wavelet is used as the basis. $\alpha_{j,k}$ can be given by

$$\alpha_{j,k} = \sigma_j\zeta_{j,k}, \tag{11}$$

where $\zeta_{j,k}$ are normalised wavelet coefficients and can be generated by stochastic OU processes as for the previous inlet. σ_j are the power coefficients and are obtained so that the power spectrum matches a desired target spectrum – again, $k^{-5/3}$.
- The final method presented here is a method based on an internal mapping. By mapping flow data from a cutting plane somewhere in the body of the computational domain, an inlet section of the domain is created in which the flow is forced to become fully developed. This is shown graphically in Fig. 1. To drive the flow, the volumetric flux of the remapped flow is checked and corrected to maintain the desired throughflow. For the test case, the mapping plane was located at a distance $x/d = 4$, i.e. two channel-widths downstream of the inlet. This represents 790 wall units of channel to develop the inlet flow; DNS and experimental results indicate that vortical streaks in near-wall flow have a separation ~100 wall units, so the remapping region resolves around seven of these structures. We will refer to this as method III – mapping method.

Fig. 3 shows time-averaged mean velocity and fluctuating velocity components plotted as profiles against distance from the wall, for various locations away from the inlet. The mean velocity profile plus the primary components of the grid scale turbulent stress are plotted, where

$$\widehat{T_{ij}} = \widehat{u_i'u_j'} \quad \text{and} \quad u_i' = u_i - \widehat{u}_i,$$

so these represent the streamwise, cross, and spanwise turbulent stresses. Also shown are results from the DNS reference data [31]. The matrix of results shows graphs at various points along the duct, from $x/d = 1$, close to the inlet itself, to $x/d = 20$ which is at the outlet. Unsurprisingly, the mean velocity profile generated for all the inlet methods is very much the same and close to the DNS data; little evolution is seen downstream of the inlet. Since the mean profile is specified for the series approaches of IIA and IIB, this profile is

Author's personal copy

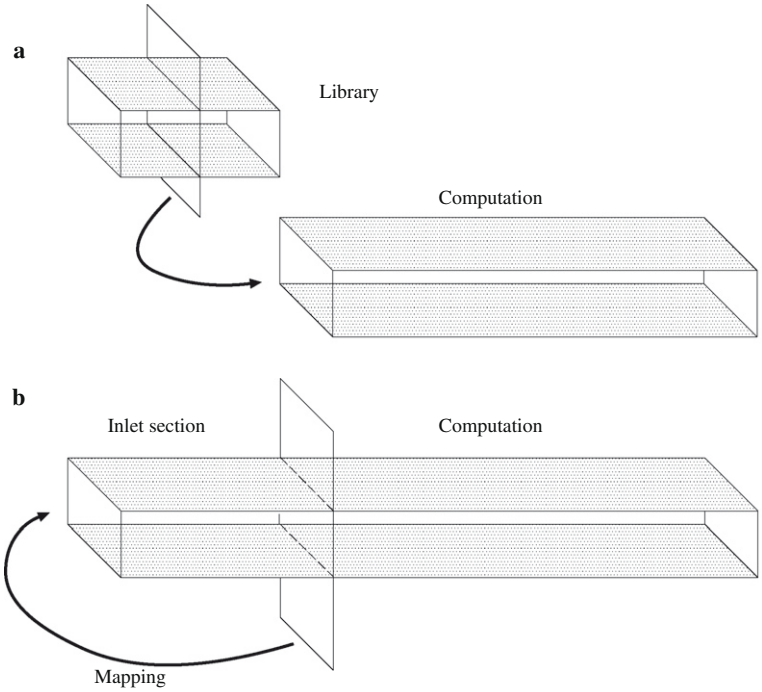

Fig. 1. Implementation of precursor simulation method (a) in which a precomputation is mined to produce inlet data, and a mapping method (b) where data is mapped back from a mid-plane section to the inlet. This generates an 'inlet section' in which the flow becomes fully developed, upstream of a 'computation' section of interest to the user.

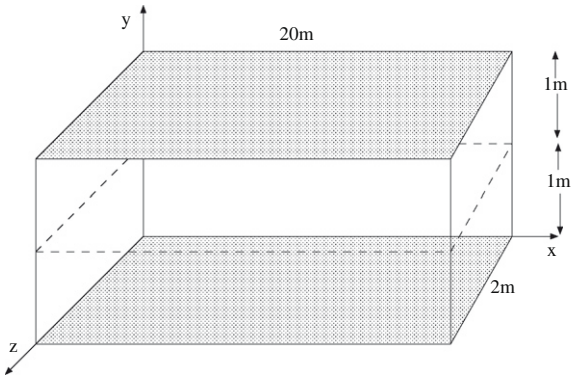

Fig. 2. Geometry for the channel; a 20 m long channel between two walls; flow is in the x-direction.

likely to be well reproduced close to the inlet for these methods, and the effect of inlet fluctuations decaying downstream will not have a direct impact upon the mean velocity profile, although it may influence it through the SGS modelling.

Of greater importance is the reproduction and evolution of the streamwise, spanwise and cross components of the stress. These parameters are of interest when LES is coupled with additional physics, particularly in combustion where velocity fluctuations around the mean have a significant impact on the flame front. As can be seen the synthesis methods (Fourier and Wavelet, IIA and IIB) are less successful at reproducing the higher order statistics, as they merely mimic the effect of turbulence rather than recreate it. This will be particularly true for T_{xy}, which represents the coupling between streamwise and spanwise fluctuating components, the effect of which is entirely absent from these inlets. The profiles evolve downstream towards the correct profile, but this is probably due to the generated inlet fluctuations evolving towards true turbulent eddies. Again, the library lookup and mapping methods are generating real turbulence and introducing this (in some form) at the inlet, and so are producing somewhat better results for the T_{xx} and T_{xy} components. The shape of the T_{yy} profiles is well reproduced, but the magnitude is over-predicted, at least initially. The precursor simulation results are not as good as the others, illustrating the issues relating to database size; the database is repeated eight times during the course of the averaging calculation. For the other methods (synthesis and mapping), longer computational runs generate more independent data which average to generate symmetric (or in the case of T_{xy}, antisymmetric) results. Fig. 4 replots Fig. 3 based on distance from the wall $y+$, using log-linear axes in order to enhance the near-wall behaviour. As expected, all models give virtually equivalent mean flow profiles; differences between the models and from the reference data are apparent for the stress components. All models generate turbulence to far out on this mesh, which is a consequence of the relatively coarse mesh used for the simulation (see below for finer mesh calculations). Comparisons between the different inlets are still valid though, and we see the best agreement with the reference channel provided by the mapping method, generating particularly good agreement for the cross-stress component T_{xy}. Note that the data from both sides of the channel has been plotted separately in this comparison, so where the results are asymmetrical for any reason (as for T_{xy}) this shows up as separate curves.

Time series data were extracted for various locations along the channel centreline and Fourier transforms evaluated to generate the spectra. Fig. 5 shows the results close to the inlet of the channel (at a position 1 m from the inlet). Figs. 6 and 7 show the spectra at x/d and x/d respectively, whilst Fig. 8 shows the results at the outlet of the long channel ($x/d = 20$). The results at $x/d = 1$ (Fig. 5) essentially demonstrate the spectrum of fluctuations generated by the inlet in each case, although it should be remarked that in the case of the mapping method this position is within the mapped section of the flow. For this position, the synthesis methods (Fourier and Wavelet) demonstrate a standard power law region which tails off at the mesh cutoff scale Δ, although with quite a wide span of fluctuations which are probably due to the discrete nature of the fluctuating modes being driven. The mapping method has gener-

Author's personal copy

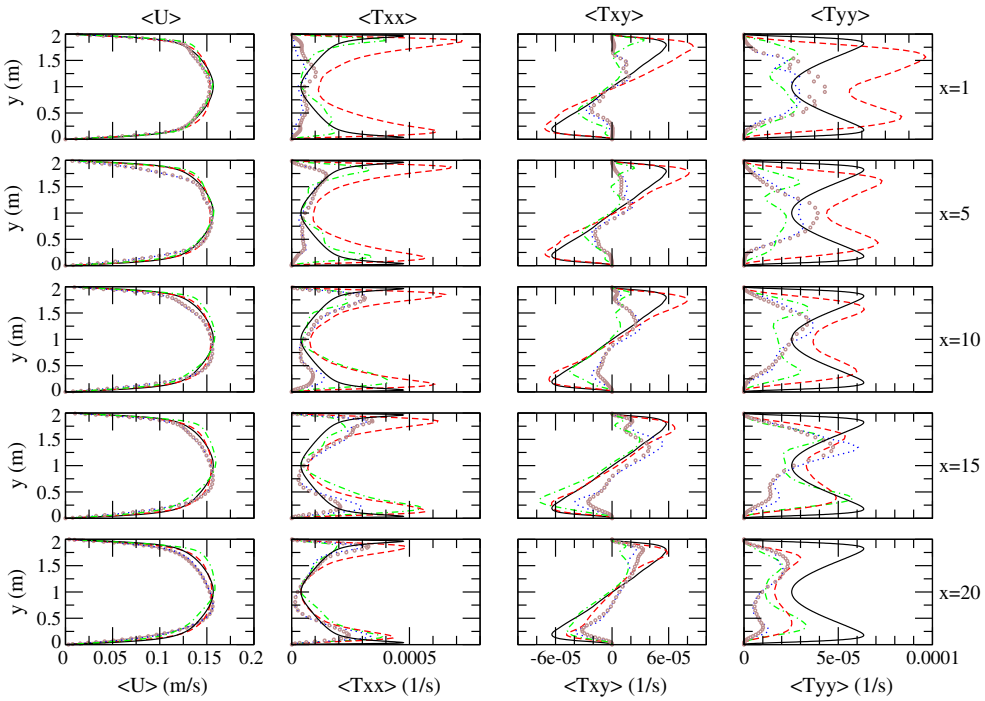

Fig. 3. Profiles of mean velocity and stress components across the channel at $x/d = 1,\ 5,\ 10,\ 15,\ 20$. Full line ≡ reference channel (DNS), dashed line ≡ mapping method, dot–dash line ≡ library look-up technique, dotted line ≡ wavelet synthesis, circle symbols ≡ Fourier synthesis.

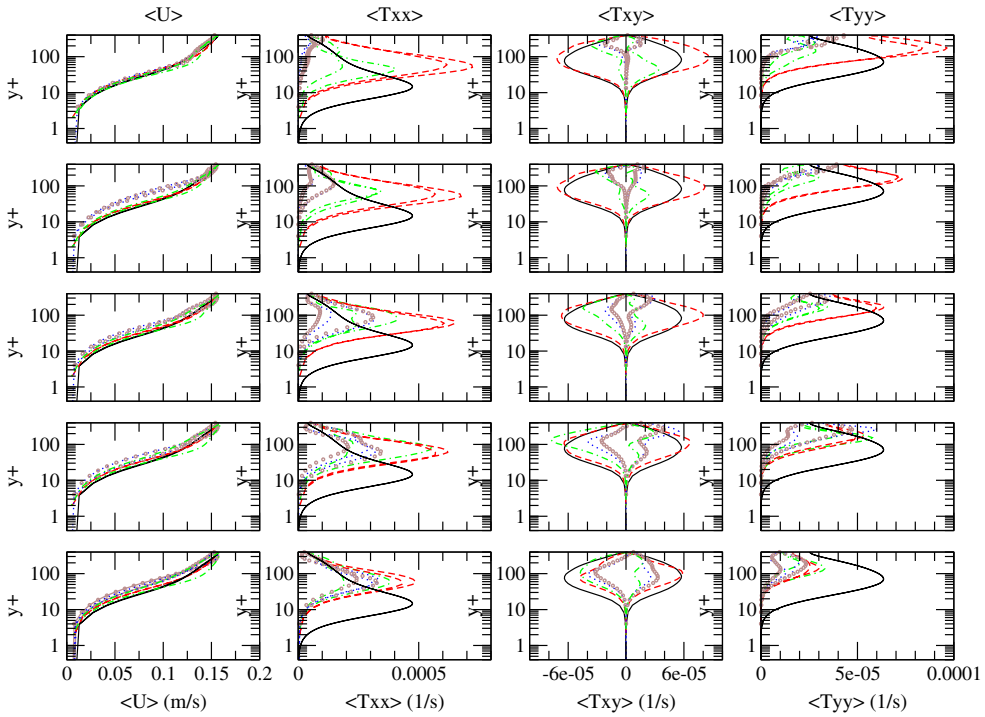

Fig. 4. Profiles of mean velocity and stress components as functions of distance $y+$ from the wall at $x/d = 1,\ 5,\ 10,\ 15,\ 20$. Full line ≡ reference channel (DNS), dashed line ≡ mapping method, dot–dash line ≡ library look-up technique, dotted line ≡ wavelet synthesis, circle symbols ≡ Fourier synthesis.

ated large (temporal) scale fluctuations, shading into a standard power law region at a lower energy level, whilst the precursor simulation method shows a flat large scale spectrum followed by a power law section including spikes. The subsequent Figs. 6–8 demonstrate the evolution of the turbulence downstream from the inlet. All simulations evolve towards a similar shaped spectrum, with considerable large (temporal) scale fluctuations, shading into a standard power law region which tails off at the mesh cutoff scale Δ. However, although the length of the channel is sufficient that some processing of the flow has occurred by the end, there are still significant variations between the results. The clearest power law spectra are given by the synthesis methods; particularly the Wave-

Author's personal copy

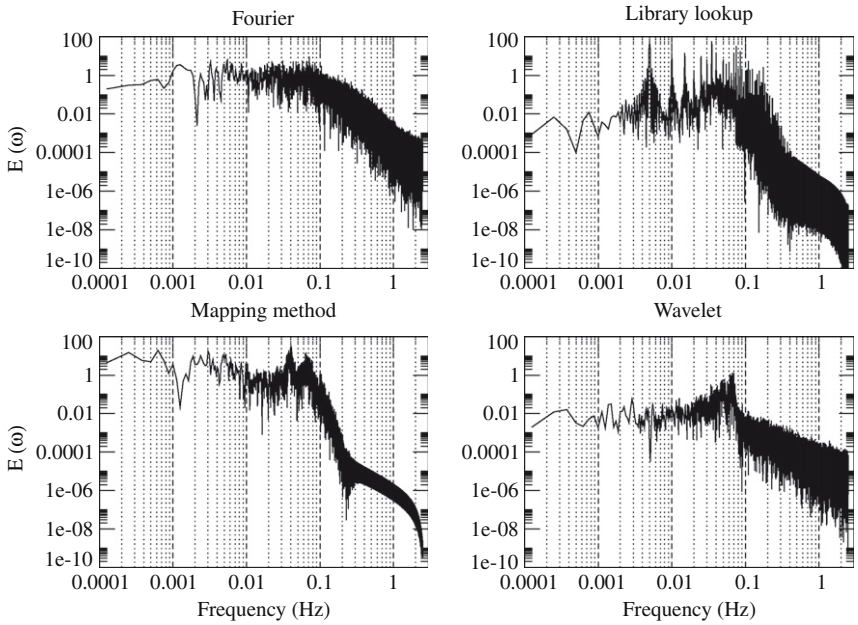

Fig. 5. Energy spectra generated from time series data $x/d = 1$ from the inlet of the channel.

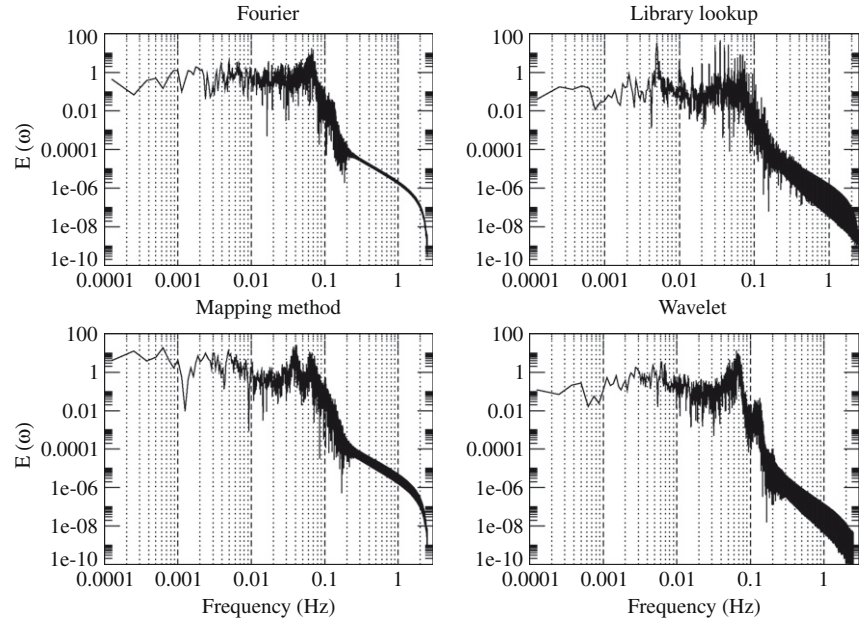

Fig. 6. Energy spectra generated from time series data at $x/d = 5$.

let method, although the slope of the spectrum is slightly greater than the expected $-5/3$ (closer to -2 in practise, possibly affected by the SGS model to some extent). The mapping method produces considerable fluctuation in the power law spectrum, whilst the precursor simulation method shows spikes in this region. Both results are probably the result of the cyclic nature of the method used to generate the turbulence in the first place. Again, the Precursor Simulation method generates a limited data set which is repeated, plausibly leading to local energy peaks at multiples of the data frequency.

Fig. 9a and b shows contour plots of enstrophy and vorticity from the various calculations. These are measures of the rotational nature of eddies in the grid scale flow, and as such provide additional information about the turbulence being generated. The plots are provided on cutting planes down the middle of the simulation domain (z = 1 m). As would be expected, the majority of the enstrophy and vorticity is being generated at the wall and diffusing into the domain from there. The library method generates results that show translational invariance down the duct, although there are also signs of periodicity in the streamwise direction. The mapping method also shows good translational invariance. The synthesis methods (Wavelet and Fourier) show a rapid decay of an initial inlet profile followed by propagation of turbulent structures into the flow from the boundary region. This is indicative of the fact that the fluctuations being generated by these methods are not true turbulence and so are being destroyed within the simulation.

As a further test, cell-volume-weighted histograms of the enstrophy have been plotted (Fig. 10) and compared with the results from a simple cyclic channel. This demonstrates the distribution of enstrophy through the volume of the simulation, and will be linked to the number and intensity of turbulent structures (i.e. eddies) within the flow. Vortical structures of considerable diameter,

Author's personal copy

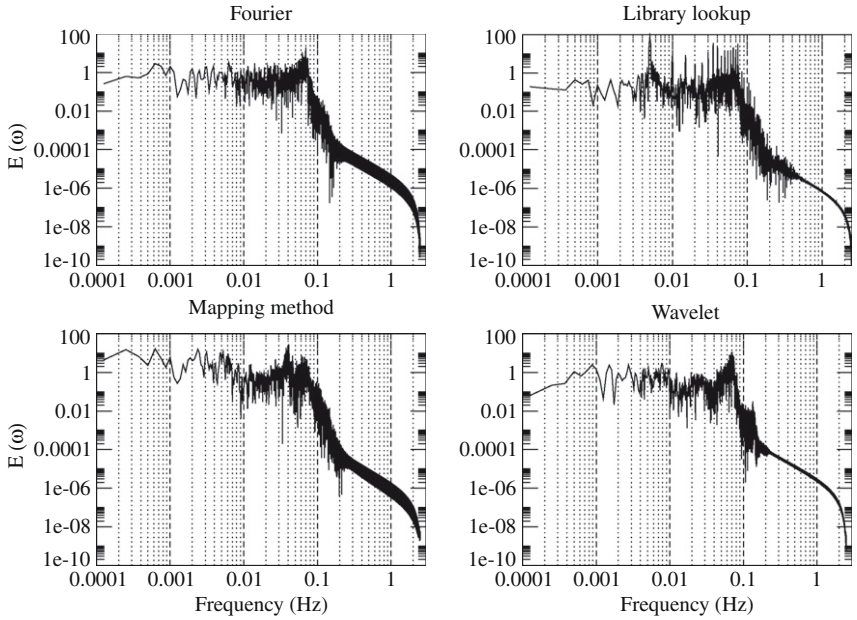

Fig. 7. Energy spectra generated from time series data at $x/d = 10$.

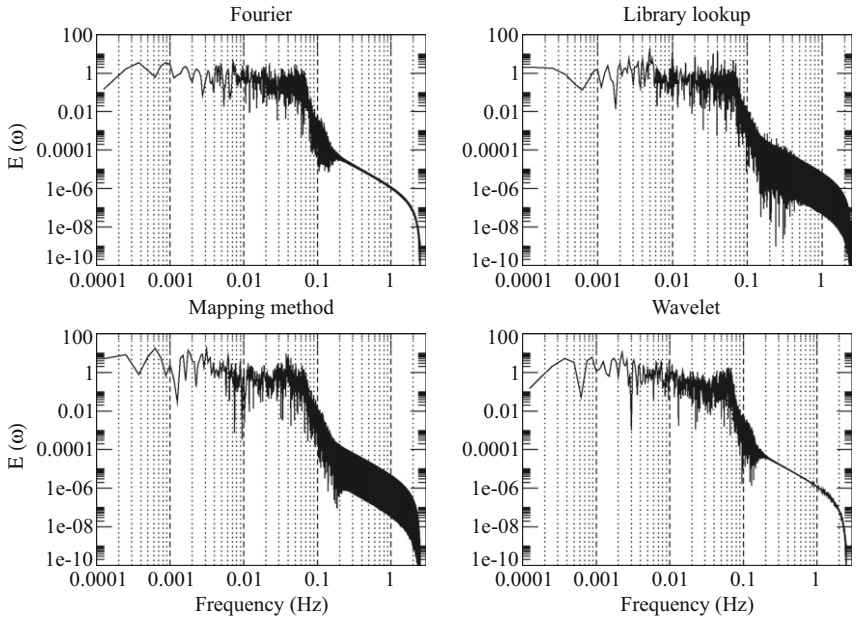

Fig. 8. Energy spectra generated from time series data at the end of the channel.

sometimes referred to as 'fat worms', have been observed before in LES [11] and *a posteriori* filtered DNS [64]. One would expect these simulations to reproduce a similar distribution of vortical structures as evidenced by the enstrophy histograms here, with a decreasing volume of space occupied by structures of increasing enstrophy. In general, this is what we find, but with the proviso that all simulations seem to be 'flatter' than would be expected, with fewer high-enstrophy regions than would be expected from comparison with the results from the cyclic channel.

5.2. Comparative discussion

In this review we have classified inlet conditions into two main categories; synthesis inlets and precursor simulation methods. The basic distinction is simple to state; synthesis techniques attempt to construct a random field at the inlet which has suitable turbulence-like properties, using mathematical processes unrelated (or not directly related) to the turbulence, whilst precursor simulation methods perform some form of explicit simulation of turbulence whose results are then utilised at the inlet to the main domain. Both approaches have some benefits to recommend them. The ideal technique would generate inlet flow which is instantly fully developed, in the sense that it should not require further processing in the main calculation to realise its turbulent nature. In reality, most methods require the provision of an inlet section in which the non-turbulent inlet fluctuations decay out but in doing so trigger the development of genuine turbulence within the domain. This is particularly the case for synthesis methods, as the issues sur-

Author's personal copy

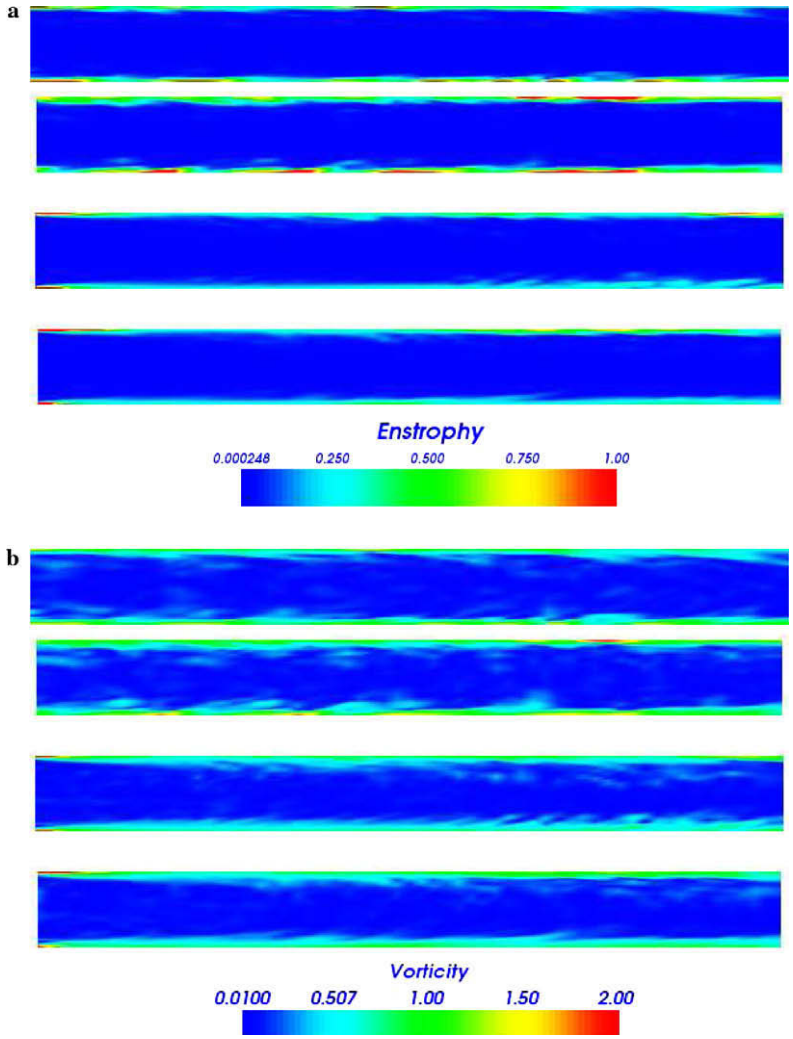

Fig. 9. (a) Enstrophy plotted on the channel centre plane. (b) Vorticity plotted on the channel centre plane. Downward from top: library method, mapping method, Wavelet synthesis method, Fourier synthesis method.

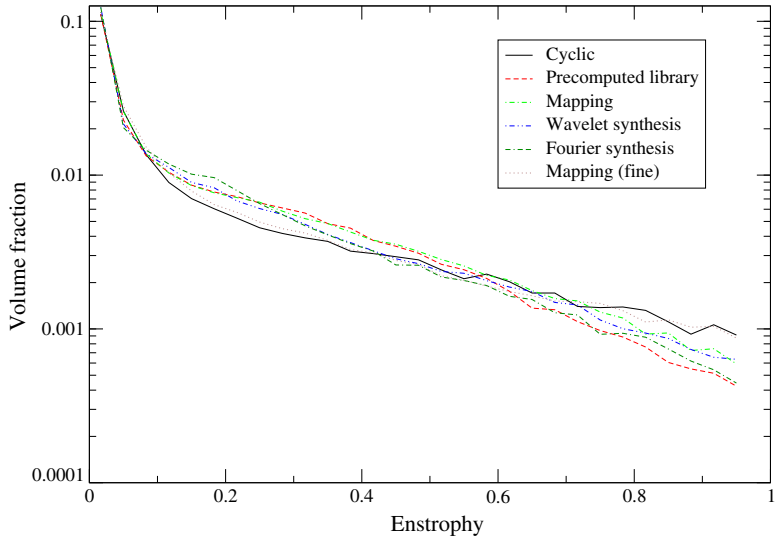

Fig. 10. Volume-weighted histogram showing the distribution of enstrophy in each calculation, compared with results from a simple cyclic channel.

Author's personal copy

rounding the generation of fluctuations with the correct correlations (spatial and temporal) make it impossible to generate a truly turbulent flow; the best that can be achieved is an inlet fluctuation which triggers the generation of turbulence in the domain with the correct statistics within as short a spatial interval as possible. However certain implementations of the library method exhibit similar problems, when the library does not match the required inlet flow conditions and has had to be processed in some way. Synthesis methods may have the advantage that they are more easily manipulated to specify the desired turbulent properties, for instance turbulent length scales or energy levels. The behaviour of the decaying inlet fluctuations may be affected by other aspects of the simulation e.g. changes in the mesh resolution in this region. It may also have a critical effect on the results, such as in the case of bypass transition on an aerofoil or turbine blade, which is known to be affected by upstream turbulent conditions [39], and flow separation for aerofoils [28]. This has significant implications for wake-passing transition in turbomachinery.

In terms of accuracy of the results, precursor simulation methods dominate; understandably as they utilise actual turbulent data. Generating this data is the sticking point with these methods. Either the data has to be taken from a preexisting source, e.g. a precomputed flow or even an experimental database, or it needs to be computed during the solution. If the data is preexisting, it may not match the desired properties – either because other data is unavailable (a turbulent flow measurement at a single Reynolds number) or because it is not possible to generate turbulent data with that particular characteristic. In this case, as observed before, it is necessary to manipulate the data to make it fit the requirements of the main simulation, which tends to destroy the benefits of using genuine turbulent data in the first place. Even if possible, the requirement of recalculating the library every time the boundary condition needs to change makes the simpler versions of this undesirable, as do the storage requirements for the library. Running the library generation concurrently with the main case and mapping the data across alleviates the storage issue and avoids problems with a statistically limited database. The most elegant solution is to combine the auxiliary calculation with the main domain, sampling the flow downstream of the inlet and reintroducing this data into the domain at the inlet.

In addition to these basic approaches, there are various methods which can be implemented to enhance the quality of the turbulent flow. Most notably are feedback control systems intended to drive the turbulent flow towards a desired result, e.g. a desired turbulence profile or mean flow condition (such as swirl). The flow can be manipulated by introducing a ficticious body force, or by explicit correction of the velocity vectors at selected points in the mesh, or in the case of recycling or cyclic methods, by mathematical transformation of the data during the mapping process. In each case, the manipulation can be linked to a metric of the flow, for example the absolute difference between the computed flow profile and the desired flow profile. For synthesis inlets, these techniques can be used to encourage the development of true turbulence within the development section, thus shortening it; coupled with the precursor simulation methods (particularly the mapping method) it can be used to drive the flow towards a specified turbulent state, e.g. non-fully developed turbulence (such as imparting a bulk swirl to the flow).

6. Conclusions

In this review we have classified inlet conditions into two main categories; synthesis inlets and precursor simulation methods. The basic distinction is that synthesis techniques attempt to construct a random field at the inlet which has suitable turbulence-like properties, whilst library methods perform some form of explicit simulation of turbulence whose results are then utilised at the inlet to the main domain. Synthesis methods make it easy to specify parameters of the turbulence, such as length scales or turbulent energy levels; they are also quick to set up and modify if conditions change. However they are inherently inaccurate and require the provision of an inlet development section during which the random fluctuations develop into true turbulence. precursor simulation methods generate true turbulence and so are inherently more accurate, however can be cumbersome to modify to generate the required state of turbulence. Merging the auxiliary calculation into the main domain as a mapping method, and using sophisticated feedback control techniques to drive the flow towards a desired state however, does make these techniques usable for LES simulations.

Acknowledgment

G.R.T., M.H.B.-A. acknowledge the support of the EPSRC through Grant GR/R27495/01.

References

[1] Abdilghanie AM, Collins LR, Caughey DA. Comparison of turbulence modeling strategies for indoor flows. J Fluids Eng 2009;131. 051402-1–051402-18.
[2] Aider J-L, Danet A. Large-eddy simulation study of upstream boundary conditions influence upon a backward-facing step flow. C.R. Mecanique 2006;334:447–53.
[3] Aider J-L, Danet A, Lesieur M. Large-eddy simulation applied to study the influence of upstream conditions on the time-dependant and averaged characteristics of a backward-facing step flow. J Turb 2007;8:N51.
[4] Andersson N, Eriksson L-E, Davidson L. Effects of inflow conditions and subgrid model on les for turbulent jets. In: 11th AIAA/CES aeroacoustics conference, May 23–5, Monterey, California; 2005.
[5] Baba-Ahmadi MH. Construction of inlet conditions for large eddy simulation. Ph.D. thesis, SECaM, University of Exeter; 2008.
[6] Baba-Ahmadi MH, Tabor G. Inlet conditions for LES of gas-turbine swirl injectors. AIAA J 2008;46(7):1782–90.
[7] Baba-Ahmadi MH, Tabor G. Inlet conditions for LES using mapping and feedback control. Comput Fluids 2009;38(6):1299–311.
[8] Batten P, Goldberg U, Chakravarthy S. Interfacing statistical turbulence closures with large-eddy simulation. AIAA J 2001;42(3):485–92.
[9] Batten P, Goldberg U, Chakravarthy S. Interfacing statistical turbulence closures with large-eddy simulation. AIAA J 2004;42:485.
[10] Benhamadouche S, Jarrin N, Addad Y, Laurence D. Synthetic turbulent inflow conditions based on a vortex method for large eddy simulation. Progr Comput Fluid Dyn 2006;6(1/2/3):50–7.
[11] Briscolini M, Santangelo P. The non-gaussian statistics of the velocity field in low-resolution large eddy simulations of homogeneous turbulence. J Fluid Mech 1994;270:199–217.
[12] Chung YM, Sung HJ. Comparative study of inflow conditions for spatially evolving simulation. AIAA J 1997;35(2):269–74.
[13] Davidson L. Hybrid LES-RANS: inlet boundary conditions. In: 3rd national conference on computational mechanics – MekIT05; 2005. p. 7–22.
[14] de Villiers E. The potential for large eddy simulation for the modelling of wall bounded flows. Ph.D. thesis, Imperial College; 2006.
[15] di Mare L, Klein M, Jones WP, Janicka J. Synthetic turbulence inflow conditions for large-eddy simulation. Phys Fluids 2006;18(2):025107.
[16] Drikakis D. Advances in turbulent flow computations using high-resolution methods. Prog Aeros Sci 2003;39:405–24.
[17] Drikakis D, Hahn M, Mosedale A, Thornber B. Large eddy simulation using high-resolution and high-order methods. Philos Trans Roy Soc A 2009;367:2985–98.
[18] Druault P, Lardeau S, Bonnet J-P, Coiffet F, Deville J, Lamballais E, et al. Generation of three-dimensional turbulent inlet conditions for large-eddy simulation. AIAA J 2004;42(3):447–56.
[19] Ferrante A, Elghobashi SE. A robust method for generating inflow conditions for direct simulations of spatially-developing boundary layers. J Comput Phys 2004;198:372.
[20] Fureby C, Gosman AD, Tabor G, Weller HG, Sandham N, Wolfshtein M. Large eddy simulation of turbulent channel flows. In: Proceedings of turbulent shear flows 11, vol. 3; 1997. p. 28.13.
[21] Fureby C, Grinstein FF, Li G, Gutmark EJ. An experimental and computational study of a multi-swirl gas turbine combustor. Proc Comb Inst 2007;31:3107–14.
[22] Fureby C, Tabor G, Weller H, Gosman AD. A comparative study of sub grid scale models in homogeneous isotropic turbulence. Phys Fluids 1997;9(5):1416–29.
[23] Fureby C, Tabor G, Weller HG, Gosman AD. Differential subgrid stress models in large eddy simulations. Phys Fluids 1997;9(11):3578–80.

Author's personal copy

[24] Fureby C, Tabor G, Weller HG, Gosman AD. Large eddy simulation of the flow around a square prism. AIAA J 2000;38(3):442–52.
[25] Garcia-Villalba M, Fröhlich J. Les of a free annular swirling jet – dependence of coherent structures on a pilot jet and the level of swirl. Int J Heat Fluid Flow 2006;27(5):911–23.
[26] García-Villalba M, Fröhlich J, Rodi W. On inflow boundary conditions for large eddy simulation of turbulent swirling jets. In: Proceedings of the 21st international congress of theoretical and applied mechanics, Warsaw, Poland; 2004.
[27] García-Villalba M, Fröhlich J, Rodi W. Identification and analysis of coherent structures in the near field of a turbulent unconfined annular swirling jet using large eddy simulation. Phys Fluids 2006;18:055103.
[28] Gilling L, Sorensen NN, Davidson L. Detached eddy simulations of an airfoil in turbulent inflow. In: 47th aerospace sciences meeting, Orlando, Florida, no. AIAA 2009-270; 2009.
[29] Grinstein FF. On integrating large eddy simulation and laboratory turbulent flow experiments. Philos Trans Roy Soc A 2009;367:2931–45.
[30] Issa RI. Solution of the implicitly discretised fluid flow equations by operator-splitting. J Comp Phys 1986;62:40–65.
[31] Iwamoto K. Database of fully developed channel flow. Technical report ILR-0201, Department of Mechanical Engineering, The University of Tokio; 2002.
[32] Jarrin N, Prosser R, Eribe J-C, Benhamadouche S, Laurence D. Reconstruction of turbulent fluctuations for hybrid rans/les simulations using a synthetic-eddy method. Int J Heat Fluid Flow 2009;30:435–42.
[33] Jasak H, Weller H, Gosman A. High resolution NVD differencing scheme for arbitrarily unstructured meshes. Int J Numer Meth Fluids 1999;31:431–49.
[34] Johansson PS, Andersson HI. Generation of inflow data for inhomogeneous turbulence. Theor Comput Fluid Dyn 2004;18:371–89.
[35] Keating A, Piomelli U, Balaras E, Kaltenbach H-J. A priori and and a posteriori tests of inflow conditions for large-eddy simulation. Phys Fluids 2004;16(12): 4696–712.
[36] Kim J, Moin P, Moser R. Turbulence statistics in fully developed channel flow at low Reynolds number. JFM 1987;177:133–66.
[37] Klein M, Sadiki A, Janicka J. A digital filter based generation of inflow data for spatially developing direct numerical or large eddy simulations. J Comput Phys 2003;186:652–65.
[38] Kondo K, Murakami S, Mochida A. Generation of velocity fluctuations for inflow boundary condition of les. J Wind Eng Ind Aero 1997;67& 68:51–64.
[39] Koyabu E, Funazaki K, Kimura M. Effects of periodic wake passing upon bypass transition of blade boundary layer and unsteady loss. In: Proceedings of the international gas turbine congress, Tokyo; 2003, p. TS–068.
[40] Kraichnan R. Diffusion by a random velocity field. Phys Fluids 1970;13:22–31.
[41] Lamballais E, Lesieur M, Métais O. Probability distribution functions and coherent structures ina turbulent channel. Phys Rev E 1997;56:6761–6.
[42] Lee S, Lele S, Moin P. Simulation of spatially evolving turbulence and the applicability of Taylor's hypothesis in compressible flow. Phys Fluids A 1992;4:1521–30.
[43] Lund TS, Wu X, Squires KD. Generation of turbulent inflow data for spatially-developing boundary layer simulations. J Comp Phys 1998;140:233–58.
[44] Mathey F, Cokljat D, Bertoglio JP, Sergent E. Assessment of the vortex method for large eddy simulation inlet conditions. Progr Comput Fluid Dyn 2006; 6(1/2/3):58–67.
[45] Patnaik G, Boris JP, Young TR, Grinstein FF. Large scale urban contaminant transport simulations with miles. J Fluids Eng 2007;129:1524–32.
[46] Perret L, Delville J, Manceau R, Bonnet J-P. Generation of turbulent inflow conditions for large eddy simulation from stereoscopic piv measurements. Int J Heat Fluid Flow 2006;27:576–84.
[47] Perret L, Deville J, Manceau R, Bonnet J-P. Turbulent inflow conditions for large-eddy simulation based on low-order empirical model. Phys Fluids 2008;20. 075107–1–17.
[48] Pierce CD, Moin P. Method for generating equilibrium swirling inflow conditions. AIAA J 1998;36:1325–7.
[49] Rhie C, Chow W. A numerical study of the turbulent flow past an isolated airfoil with trailing edge separation. AIAA J 1983;21(7):1225–32.
[50] Schlüter JU, Pitsch H, Moin P. Boundary conditions for les in coupled simulations. Technical report AIAA-2003-0069, 41st aerospace sciences meeting; January 6–9, 2003.
[51] Schlüter JU, Pitsch H, Moin P. Large eddy simulation inflow conditions for coupling with Reynolds-averaged flow solvers. AIAA J 2004;42(3):478–84.
[52] Sergent ME. Vers une méthodologie de couplage entre la simulation des grandes echelles et les modèles statistiques. Ph.D. thesis, Ecole Central de Lyon; 2002.
[53] Smirnov A, Shi S, Celik I. Random flow generation technique for large eddy simulations and particle-dynamics modelling. J Fluids Eng 2001;123:359–71.
[54] Spalart P, Jou W-H, Strelets M, Allmaras S. Comments on the feasibility of les for wings, and on a hybrid rans/les approach. In: Liu C, Liu Z, editors. Advances in DNS/LES. Greyden Press; 1997.
[55] Spalart PR. Numerical study of sink-flow boundary layers. J Fluid Mech 1986;172:307.
[56] Spalart PR. Direct simulation of a turbulent boundary layer up to $r_\theta = 1410$. JFM 1988;187:61–98.
[57] Spalart PR, Watmuff JH. Experimental and numerical study of a turbulent boundary layer with pressure gradients. J Fluid Mech 1993;249:337–71.
[58] Spille-Kohoff A, Kaltenbach H-J. Generation of turbulent inflow data with a prescribed shear–stress profile. In: Liu C, Sakell L, Beutner T, editors. DNS/LES progress and challenges. Columbus (OH): Greydon; 2001.
[59] Szbrizzai F, Verzicco R, Soldati A. Turbulent flow and dispersion of inertial particles on a confined jet issued by a long cylindrical pipe. Flow Turb Combust 2009;82:1–23.
[60] Tabor G, Baba-Ahmadi MH, de Villiers E, Weller HG. Construction of inlet conditions for LES of turbulent channel flow. In: Proceedings of the ECCOMAS congress, Jyväskylä, Finland; 2004.
[61] Temmerman L, Leschziner MA, Mellen C, Froehlich J. Investigation of wall-function approximations and subgrid scale models in large eddy simulation of separated flow in a channel with streamwise periodic constrictions. Int J Heat Fluid Flow 2002;24:157–80.
[62] Veloudis I, Yang Z, McGuirk JJ, Page GJ. Assessment of digital filter approach for generating large eddy simulation inlet conditions. In: Rodi W, Mulas M, editors, Proceedings of ETMM 6, Sardinia, Italy, Elsevier, Amsterdam, The Netherlands; 2005. p. 307–16.
[63] Veloudis I, Yang Z, McGuirk JJ, Page GJ, Spencer A. Novel implementation and assessment of a digital filter based approach for the generation of les inlet conditions. Flow Turb Combust 2007;79:1–24.
[64] Vincent A, Meneguzi M. The spatial structure and statistical properties of homogeneous turbulence. J Fluid Mech 1994;225:1.
[65] Wang P, Bai X. Large eddy simulations of turbulent swirling flows in a dump combustor: a sensitivity study. Int J Numer Meth Fluids 2005;47:99–120.
[66] Wang P, Bai XS, Wessman M, Klingmann J. Large eddy simulation and experimental studies of a confined turbulent swirling flow. Phys Fluids 2004;16(9):3306–24.
[67] Xie Z-T, Castro IP. Efficient generation of inflow conditions for large eddy simulation of street-scale flows. Flow Turb Comb 2008;81:449–70.